Discriminative Analysis for Symmetric Positive Definite Matrices on Lie Groups

Chunyan Xu, Canyi Lu, Junbin Gao, Wei Zheng, Tianjiang Wang, and Shuicheng Yan

***Abstract*— In this paper, we study discriminative analysis of symmetric positive definite (SPD) matrices on Lie groups (LGs), namely, transforming an LG into a dimension-reduced one by optimizing data separability. In particular, we take the space of SPD matrices, e.g., covariance matrices, as a concrete example of LGs, which has proved to be a powerful tool for high-order image feature representation. The discriminative transformation of an LG is achieved by optimizing the within-class compactness as well as the between-class separability based on the popular graph embedding framework. A new kernel based on the geodesic distance between two samples in the dimension-reduced LG is then defined and fed into classical kernel-based classifiers, e.g., support vector machine, for various visual classification tasks. Extensive experiments on five public datasets, i.e., Scene-15, Caltech101, UIUC-Sport, MIT-Indoor, and VOC07, well demonstrate the effectiveness of discriminative analysis for SPD matrices on LGs, and the state-of-the-art performances are reported.**

***Index Terms*— Discriminative analysis, graph embedding, Lie group (LG), visual classification.**

I. Introduction

THE past few decades have witnessed significant growth in the utilization of structured data in various computer vision and machine-learning applications [2]–[4], where richer representations of data, such as matrices, tensors, or graphs, are utilized instead of typical vector spaces. One of the interesting data structures that have gained much attention recently is symmetric positive definite (SPD) matrices, the space of which is known to form a Lie group (LG) [5]–[7]. A LG is a group with the structure of a differentiable manifold such that the group operations, multiplication and inverse, are differentiable maps. The SPD matrices provide a powerful platform for analyzing visual signals, such as images and videos.

Due to their great importance in computer vision literature, SPD matrices have been much researched. A popular kind of SPD image descriptors, namely, region covariance [8], is a powerful tool for encoding second-order image features and has been applied to object detection and texture classification. To address the semantic segmentation problem, Carreira *et al.* [9] took advantage of the manifold structure of SPD matrices to analyze a certain kind of second-order statistics of image features.

The SPD matrices are mapped to a high-dimensional Hilbert space by kernels and applied to pedestrian detection, image segmentation, and object categorization [6]. To employ the geometric structure of SPD matrices, Li *et al.* [7] also proposed a kernel-based method for sparse representation and dictionary learning on LGs and applied it to scene categorization, texture classification, and face recognition.

Although SPD matrices have been proved to be a powerful tool for visual feature representation, successful applications still suffer from two limitations.

1) Without considering the local structure of data on LGs, the discrimination may be adversely affected by some outliers and multimodal classes may adversely affect the discrimination.
2) Due to the redundancy of the manifold-valued data, its discriminative power may also be limited.

To overcome the above limitation, a possible way is to perform discriminative analysis to reduce the dimension of the SPD matrices as in the Euclidean subspace.

To address these issues, we propose a novel method in this paper called discriminative analysis for SPD matrices on LGs, namely, transforming an LG to a dimension-reduced one by optimizing data separability. In particular, we learn a discriminative transformation between two LGs based on the popular graph embedding framework [1]. First, two graphs are defined, i.e., an intrinsic graph and a penalty graph. The intrinsic graph characterizes the within-class compactness and connects points of the same class, while the penalty graph characterizes the between-class separability and connects the marginal points of different classes. Then a discriminative transformation is learned by enhancing the within-class compactness as well as maximizing the between-class separability. As a by-product, our proposed algorithm also reduces the dimensionality of SPD matrices, which will reduce the cost of model training and test in the pattern analysis. Finally, a new kernel based on the geodesic distance between two points in the dimension-reduced LG is then defined and fed into classical

Manuscript received May 5, 2014; revised August 28, 2014 and October 31, 2014; accepted January 8, 2015. Date of publication January 19, 2015; date of current version September 30, 2015. This work was supported in part by the National Natural Science Foundation of China under Grant 61073094 and Grant U1233119 and in part by the Australian Research Council through the Discovery Projects under Project DP140102270. This paper was recommended by Associate Editor X. Li.

C. Xu is with the School of Computer Science and Technology, Huazhong University of Science and Technology, Wuhan 430074, China, and also with the National University of Singapore, Singapore 119077 (e-mail: xuchunyan01@gmail.com).

C. Lu and S. Yan are with the Department of Electrical and Computer Engineering, National University of Singapore, Singapore 119077.

J. Gao is with the School of Computing and Mathematics, Charles Sturt University, Bathurst, NSW 2795, Australia.

W. Zheng is with the Beijing Samsung Telecom Research and Development Center, Beijing 214020, China.

T. Wang is with the School of Computer Science and Technology, Huazhong University of Science and Technology, Wuhan 430074, China.

Color versions of one or more of the figures in this paper are available online at http://ieeexplore.ieee.org.

Digital Object Identifier 10.1109/TCSVT.2015.2392472

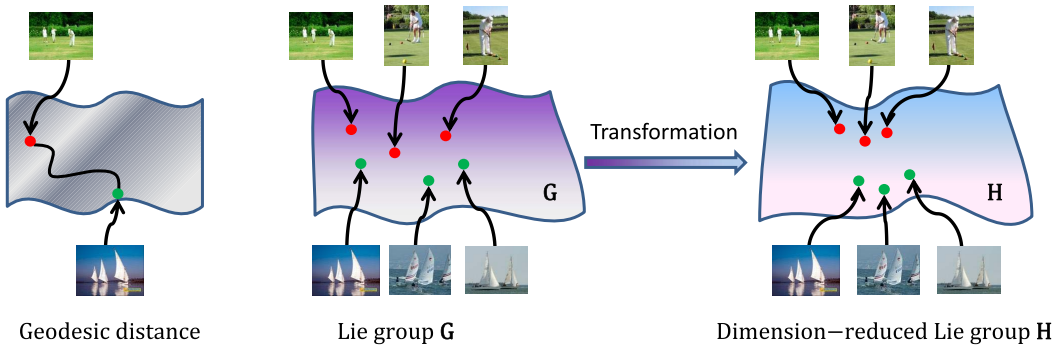

Fig. 1. Discriminative analysis for SPD matrices on LGs. SPD matrices are embedded as points on the LG, and the geometric distance between two points can be computed. Our proposed algorithm transforms the data points from a LG **G** into a dimension-reduced one **H** by optimizing data separability. Specifically, the connected points with the same label stay as close together as possible, while connected points sharing different labels stay as far away as possible. Example images are from the UIUC-Sport database [10].

kernel-based classifiers, e.g., support vector machine (SVM), for various visual classification tasks. Taking the UIUC-Sport event classification as an example, Fig. 1 shows the framework of the discriminative analysis for SPD matrices on LGs.

The remainder of this paper is organized as follows. In Section II, we will review some related work. Section III introduces the background knowledge about LG. Section IV describes the discriminative analysis on LGs and also presents how to solve the induced optimization problem. In Section V, we apply our approach to visual classification, followed by the experimental results and algorithm analysis in Section VI. The main findings and possible future research are summarized in Section VII.

II. Related Work

We recall some standard similarity measures for SPD matrices. The distance or similarity measure over the space of SPD matrices is crucial for discriminative analysis. A simple method is to represent $n \times n$ SPD matrices as vectors in $\mathbb{R}^{(d\times(d+1)/2)}$, and then the distance in the Euclidean space can be used [9]. However, the space of SPD matrices does not conform with the Euclidean geometry, but forms an LG that is a differentiable manifold. Vectorizing the covariances into the Euclidean space ignores the manifold structure, which leads to poor performance [11].

A better choice is to consider the curvature of the Riemannian manifold and use the corresponding geodesic length along the manifold surface as the distance. Several different similarity measures or metrics of SPD matrices have been proposed. For X_i, X_j in S_n^+, the affine-invariant Riemannian metric (AIRM) [12] is defined as $D_{\text{AIRM}} = ||\log(X_i^{-1/2} X_j X_i^{-1/2})||_F$. This metric enjoys several useful theoretical properties, but its computational complexity for lager matrices causes significant slow-downs. The Jensen–Bregman LogDet Divergence (JBLD) [13] is defined as $D_{\text{JBLD}} = \log|(X_i + X_j/2)| - (1/2)\log|X_i X_j|$, where $|\cdot|$ denotes the determinant. Although the computational speed of JBLD metric is fast, the structure of the manifold space may not be preserved well. Wang and Vemuri [14] proposed the J divergence as the distance measure for SPD matrices, $D_{\text{Jdiv}}(X_i, X_j) = ((1/2)\text{tr}(X_i^{-1}X_j + X_j^{-1}X_i) - n)^{1/2}$, where $\text{tr}(\cdot)$ is the matrix trace operator and n is the size of square matrix X_i and X_j. In addition, the symmetrized Kullback-Leibler-divergence metric (KLDM) [2] is defined, $D_{\text{KLDM}}(X_i, X_j) = (1/2)\text{tr}(X_i^{-1}X_j + X_j^{-1}X_i - 2I)$. The J-divergence [14] and KLDM metric [2] require the inversion of the SPD matrices, which can be slow, and may lead to poor accuracy with overestimating the Riemannian metric.

The log-Euclidean Riemannian metric (LERM) is defined as

$$D_{\text{LE}}(X_i, X_j) = \|\log(X_i) - \log(X_j)\|_F \tag{1}$$

where $X_i, X_j \in \mathcal{S}_n^+$, $\mathcal{S}_n^+$ denotes the set of SPD matrices with size $n \times n$, $\log(\cdot)$ is the principal matrix logarithm, and $\|\cdot\|_F$ denotes the Frobenius norm of a matrix. The log-Euclidean mapping $\log(X)$ maps the SPD matrix to a flat Riemannian space, and thus the Euclidean distances can be used in LERM, which are widely used due to their easy computation and several important properties, e.g., invariance to inversion and similarity transforms. For the pedestrian detection problem, Tuzel *et al.* [15] utilized SPD matrices as object descriptors and implemented the boosting method on the Riemannian manifold. Vemulapalli *et al.* [16] performed classification by mapping SPD matrices from Riemannian manifolds to the Euclidean spaces using the kernel learning approach. We also used the LERM in this paper.

The conventional discriminative analysis methods, e.g., linear discriminant analysis (LDA) [17] and marginal Fisher analysis (MFA) [1], do not consider the LG geometric structure of the data, which may result in the loss of important discriminative information. Moreover, it is difficult to carry out the discriminative analysis on LGs as the conventional vector-based discriminative analysis methods.

There have also been considerable research efforts [18] devoted to discriminative analysis for the Riemannian manifolds such as the Grassmann manifold. Hamm and Lee [19] performed the discriminant analysis using kernel LDA with the Grassmann kernels, but only focused on the manifold kernel LDA to classification problems. Harandi *et al.* [20] also proposed a graph embedding discriminative analysis on the Grassmann manifold, which maps the manifold space into the reproduced kernel Hilbert spaces.

Recently, Li *et al.* [21] embedded the space of Gaussian into the space of SPD matrices, which are analyzed from the LG manifold point of view. To get a discriminative distance, they attempted to find a linear transformation in the logarithm domain, which is defined as

$$D(X_i, X_j) = \mathrm{tr}\big((\log(X_i) - \log(X_j))^T M(\log(X_i) - \log(X_j))\big) = ||A(\log(X_i) - \log(X_j))||_F \quad (2)$$

where X_i, X_j, and M are the three SPD matrices with size $n \times n$, and $M = A^T A$. Wang *et al.* [22] proposed a discriminative learning approach by modeling the image set with SPD matrices and also explored the log-Euclidean distance metric for SPD matrices. With this metric function, they can map the SPD matrix from the Riemannian manifold to an Euclidean space, and then some learning methods (such as LDA and partial least squares) with respect to the vector space can be exploited in linear/kernel formulation.

From the perspective of distance metrics, our proposed method is also based on the same LERM with [21] and can also be seen as a kind of metric learning method on the LG manifold space. However, these manifold discriminative analysis methods, which are based on a metric learning view of the problem, perform the following.

1) They do not tackle subspace learning between the manifold spaces, but transform the manifold space to the vector space.
2) They also suffer from the redundancy of the manifold-valued data, namely, not transforming an LG to a dimension-reduced one.

III. Background Knowledge of Lie Group

A. Lie Groups and Lie Algebra

An LG $\mathbf{G}$ is a smooth manifold with a group structure, in which the group operations of multiplication and inversion are smooth maps [23]. In particular, the group is characterized by a unique identity element $I \in \mathbf{G}$ and two group operations

$$\text{multiplication } g_1 g_2 : \mathbf{G} \times \mathbf{G} \to \mathbf{G}, \quad \text{inversion } g^{-1} : \mathbf{G} \to \mathbf{G} \quad (3)$$

which are smooth mappings.

The tangent space of the LG $\mathbf{G}$ to its identity element I forms a Lie algebra $\mathfrak{g}$. We can map between the LG and its tangent space from the identity element I using the exponential and logarithmic maps

$$\bar{X} = \log(X), \quad X = \exp(\bar{X}) \quad (4)$$

where $X \in \mathbf{G}$ and $\bar{X} \in \mathfrak{g}$ are the elements of LG and Lie algebra, respectively. In this paper, we only focus on the matrix LGs. The exponential and logarithm maps of a matrix are given by

$$\log(X) = \sum_{i=1}^{\infty} \frac{(-1)^{i-1}}{i}(X - I)^i, \quad \exp(\bar{X}) = \sum_{i=0}^{\infty} \frac{1}{i!}\bar{X}^i. \quad (5)$$

Let $\mathbf{G}$ and $\mathbf{H}$ be the LGs with their corresponding Lie algebras $\mathfrak{g}$ and $\mathfrak{h}$. A transformation $\phi : \mathbf{G} \to \mathbf{H}$ from a LG $\mathbf{G}$ to $\mathbf{H}$ is called a smooth map if it is a group homomorphism [24]. That is to say, the LG homomorphism is a map between LGs $\phi : \mathbf{G} \to \mathbf{H}$, which is both a group homomorphism and a smooth map. ϕ_* is a map between the corresponding Lie algebras $\mathfrak{g}$ and $\mathfrak{h}$: $\phi_* : \mathfrak{g} \to \mathfrak{h}$. The maps ϕ and ϕ_* are related by the exponential maps. For any $\bar{X} \in \mathfrak{g}$, we have

$$\phi(\exp(\bar{X})) = \exp(\phi_*(\bar{X})). \quad (6)$$

B. $\mathcal{S}_n^+$ as a Lie Group

$\mathcal{S}_n^+$ is a LG with the identity element being the identity matrix I and its inverse operation follows the regular matrix inversion. In the log-Euclidean framework, the logarithmic multiplication $\odot : \mathcal{S}_n^+ \times \mathcal{S}_n^+ \mapsto \mathcal{S}_n^+$ and the inversion are defined as [5]

$$X_i \odot X_j := \exp(\log(X_i) + \log(X_j)) \quad X_i^{-1} := \exp(-\log(X_i)). \quad (7)$$

It can be seen that the multiplication operation and inverse operation are smooth mappings in the log-Euclidean framework. Therefore, the space of $\mathcal{S}_n^+$ forms a LG.

The distance of two points on a LG can be measured by the shortest length of the curve connecting them. The minimum length curve between two points is called the geodesic. With the above logarithm map and the group operation, the geodesic distance [5], [23] between two elements on a LG can be computed by

$$D_{\mathrm{LE}}(X_i, X_j) = ||\log(X_i) - \log(X_j)||_F \quad (8)$$

where X_i and $X_j \in \mathcal{S}_n^+$ and $||\cdot||_F$ denote the Frobenius norm of a matrix.

IV. Discriminative Analysis for SPD Matrices

In this section, we introduce discriminative analysis for SPD matrices on LGs, namely, transforming a LG $\mathbf{G}$ into a dimension-reduced one $\mathbf{H}$ by optimizing data separability. Under the popular graph embedding framework [1], we learn the discriminative transformation between LGs, by introducing intrinsic and penalty graphs to, respectively, characterize within-class compactness and between-class separability.

A. Transformation Between Lie Groups

Let $X_i \in \mathcal{S}_m^+$ and $Y_i \in \mathcal{S}_n^+$ (usually $n < m$) be two points on two LGs $\mathbf{G}$ and $\mathbf{H}$, respectively. According to the LG homomorphism theory [24], we introduce a transformation from a LG $\mathbf{G}$ to another LG $\mathbf{H}$, i.e., $\phi : X_i \to Y_i$. The tangent spaces of LGs $\mathbf{G}$ and $\mathbf{H}$ to the identity element I form the Lie algebras $\mathfrak{g}$ and $\mathfrak{h}$, respectively. The LG and the corresponding Lie algebra space can be mapped using the exponential and logarithmic maps, i.e., $\mathbf{G} = \exp(\mathfrak{g})$ and $\mathfrak{g} = \log(\mathbf{G})$.

In the Lie algebra space, $\bar{X}_i \in \mathfrak{h}$, $\bar{Y}_i \in \mathfrak{g}$ are, respectively, two points corresponding to $X_i \in \mathbf{G}$ and $Y_i \in \mathbf{H}$ by the exponential and logarithmic maps

$$\bar{X}_i = \log(X_i), \quad X_i = \exp(\bar{X}_i) \quad \bar{Y}_i = \log(Y_i), \quad Y_i = \exp(\bar{Y}_i). \quad (9)$$

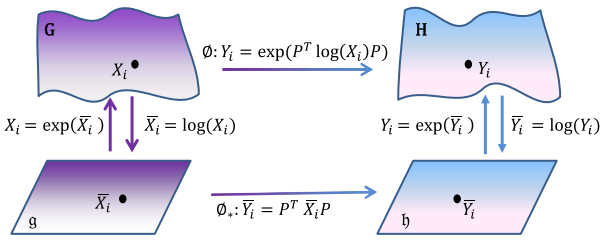

Fig. 2. Transformation between LGs. The tangent spaces of LGs **G** and **H** to the identity element I form the Lie algebras $\mathfrak{g}$ and $\mathfrak{h}$, respectively. The LG and the corresponding Lie-algebra space can be mapped using the exponential and logarithmic maps. The map between the Lie algebras ($\mathfrak{g} \to \mathfrak{h}$) is denoted by ϕ_*: $\bar{Y}_i = P^T \bar{X}_i P$. Then we can get the transformation from one LG **G** to another LG **H**, ϕ: $Y_i = \exp(P^T \log(X_i)P)$.

It can be seen from (9) that $\bar{X}_i$ is symmetric and with the same size as X_i. $\bar{Y}_i$ is also symmetric and with the same size as Y_i. Instead of defining the transformation $\phi : X_i \to Y_i$ between the LGs **G** and **H** directly, we define the transformation $\phi_* : \bar{X}_i \to \bar{Y}_i$ between their corresponding Lie algebras $\mathfrak{h}$ and $\mathfrak{g}$ as

$$\phi_* : \ \bar{Y}_i = P^T \bar{X}_i P \tag{10}$$

where $P \in \mathbb{R}^{m \times n}$. Multiplying P^T and P on both sides of $\bar{X}_i$ preserves the symmetric structure of the data.

Based on the mapping (9) between the LGs and their corresponding Lie algebras using the exponential and logarithmic map, the corresponding transformation from the LG **G** to **H** is

$$\begin{aligned} \phi : \ Y_i &= \exp(\bar{Y}_i) \\ &= \exp(P^T \bar{X}_i P) \\ &= \exp(P^T \log(X_i) P). \end{aligned} \tag{11}$$

According to the above LG transformation ϕ, all such points X_i on the LG **G** can be mapped to other points Y_i in the set **H**. It can be proved that **H** also forms a LG by the definition directly. Actually, the multiplication and inversion operations of the elements (Y_i, $Y_j \in \mathbf{H}$) are

$$\begin{aligned} Y_i \odot Y_j : &= \exp(\log(Y_i) + \log(Y_j)) \\ &= \exp(P^T \log(X_i) P + P^T \log(X_j) P) \\ &= \exp(P^T (\log(X_i) + \log(X_j)) P), \\ Y_i^{-1} : &= \exp(-\log(Y_i)) \\ &= \exp(-P^T \log(X_i) P). \end{aligned} \tag{12}$$

Since X_i and X_j are the SPD matrices, it is easy to be verified that both $Y_i \odot Y_j$ and Y_i^{-1} are the SPD matrices. By the definition of the LG, all the projected points Y_i form a LG **H**. Fig. 2 shows how to construct the transformation between the LGs.

B. Discriminative Learning for SPD Matrices on Lie Groups

In this section, we present the discriminative analysis for SPD matrices on the LGs to improve the discriminative power of the data. Specifically, we aim to learn a discriminative transformation from a LG into a dimension-reduced one by optimizing data separability. The discriminative transformation of the LG is achieved by enhancing the within-class compactness as well as maximizing the between-class separability based on the popular graph embedding framework in [1].

Based on the MFA method [1], we design the intrinsic graph and the penalty graph for our proposed algorithm. The intrinsic graph W^w characterizes the within-class compactness and connects each data point with its neighboring points of the same class, while the penalty graph W^b characterizes the between-class separability and connects the marginal point pairs of different classes.

Suppose we are given N labeled points $\{X_i, l_i\}_{i=1}^N$ from the underlying LG **G**, where $X_i \in \mathcal{S}_n^+$ and $l_i \in \{1, 2, \ldots, C\}$ with C denoting the number of classes. The local space structure of the LG can be modeled by building the intrinsic graph W^w and the penalty graph W^b. Based on the within-class compactness and the between-class separability, W^w and W^b are, respectively, defined by

$$\begin{aligned} W_{ij}^w &= \begin{cases} 1, & \text{if } X_i \in N_{k_1}^+(X_j) \text{ or } X_j \in N_{k_1}^+(X_i) \\ 0, & \text{otherwise} \end{cases} \\ W_{ij}^b &= \begin{cases} 1, & \text{if } (X_i, X_j) \in P_{k_2}(c_i) \text{ or } (X_i, X_j) \in P_{k_2}(c_j) \\ 0, & \text{otherwise} \end{cases} \end{aligned} \tag{13}$$

here, $N_{k_1}^+(X_i)$ indicates the index set of the k_1 nearest neighbors of the sample X_i in the same class, π_c denotes the index set of samples belonging to the cth class, $P_{k_2}(c)$ is the set of the k_2 nearest data pairs among the set $\{(X_i, X_j), X_i \in \pi_c, X_j \notin \pi_c\}$, and the nearest neighbors of the samples are computed by the distance metric in (8).

To further improve the discriminative power on the LGs and preserve the geometrical structure of the data, we perform discriminative analysis by simultaneously characterizing the within-class compactness and the between-class separability. In other words, the connected points of W^w stay as close together as possible, while connected points of W^b stay as distant as possible. Then we can describe the above analysis by optimizing the following two objective functions:

$$\begin{aligned} \min_P f_1 &= \sum_{i,j} D_{\text{LE}}(Y_i, Y_j)^2 W_{ij}^w \\ &= \sum_{i,j} ||\log(Y_i) - \log(Y_j)||_F^2 W_{ij}^w \end{aligned} \tag{14}$$

$$\begin{aligned} \max_P f_2 &= \sum_{i,j} D_{\text{LE}}(Y_i, Y_j)^2 W_{ij}^b \\ &= \sum_{i,j} ||\log(Y_i) - \log(Y_j)||_F^2 W_{ij}^b \end{aligned} \tag{15}$$

where $Y_i = \exp(P^T \log(X_i) P)$ and $\log(Y_i) = P^T \log(X_i) P$, and the proof of Equations (14) and (15) can be seen in Appendix A. Equation (14) punishes the neighbors in the same class if they are mapped far away on the new LG **H**, while (15) punishes the points of different classes if they are mapped close together on the new LG **H**. By converting both problems into minimization, the overall optimization problem is[1]

$$P^* = \arg\min_P (f_1 - f_2). \tag{16}$$

[1]One may use other objective functions to learn the transformation, e.g., $\min(f_1/f_2)$. For the convenience of the optimization, we simply use (16).

Algorithm 1 Discriminative Analysis for SPD Matrices on LGs

Input: Training set $\{X_i, l_i\}_{i=1}^N$ from underlying LG $\mathbf{G}$, where $X_i \in \mathcal{S}_n^+$, and $l_i \in \{1, 2, \ldots, C\}$, with C denoting the number of classes.

1: Construct intrinsic graph W^w and penalty graph W^b with (13).
2: Solve problem (16) for learning a discriminative transformation.
3: Transform all points from a LG $\mathbf{G}$ to another dimension-reduced LG $\mathbf{H}$ by (11).

The whole procedure of our proposed algorithm is outlined in Algorithm 1.

Differentiating $f_1 - f_2$ with respect to the transformation matrix P yields a gradient rule which will be used for optimization

$$\frac{\partial(f_1 - f_2)}{\partial P} = 8 \sum_{i,j} \big(\log(X_i) P P^T \log(X_i) P - \log(X_i) P P^T \log(X_j) P \big) \big(W_{ij}^w - W_{ij}^b \big) \quad (17)$$

where its proof can be seen in Appendix B. In minimizing the criterion in (16), we can calculate (17) and update the transformation matrix P by a conjugate gradients optimizer (like the neighborhood components analysis method [25])

$$P_{t+1} = P_t - \epsilon \frac{\partial(f_1 - f_2)}{\partial P_t} \quad (18)$$

where ϵ is the step size in the gradient descent. Furthermore, by restricting P to be a nonsquare matrix of $m \times n$ ($n < m$), the data dimension is reduced after the transformation by the discriminative analysis for SPD matrices. Furthermore, to optimize the transformation matrix P in (16), we employ a conjugate gradient optimizer that is a standard optimization method [26], and as a result, the transformation matrix P can only obtain a local minimum in the sense of (16), which will again be shown in the experimental parts.

We finally perform a rigorous theoretical complexity analysis of the proposed algorithm. For the per-iteration with (17), the computational complexity is about $\mathcal{O}(N^2 m^2 n)$, where N is the number of image samples in the training set, m and n are the sizes of the square matrices X_i and Y_i, respectively. For mapping each SPD matrix from the LG manifold to the Euclidean space, the complexity of computing $\log(X_i)$ is $\mathcal{O}(n^3)$, where n is the size of a square matrix X_i. Therefore, for computing similarity matrix with (8), the computational complexity is $\mathcal{O}(Nn^3)$.

V. Application for Visual Classification

To evaluate our proposed algorithm, we apply it for visual classification and introduce how to extract SPD descriptors for visual images. Recently, Carreira *et al.* [9] mapped SPD local descriptors to the tangent space using the theory of log-Euclidean metrics, but they just constructed the feature vector from the upper triangle of $\log(X_i)$, and then obtained the distance by the inner product between feature vectors. Inspired by the second-order feature pooling algorithm [9], we utilize this SPD descriptor for the visual classification problem.

We use the second-order image feature pooling algorithm [9] to extract the second-order feature with a spatial pyramid scheme [27]. For an image i, the SPD descriptor of an image region R_k can be defined as

$$X_{ik} = \frac{1}{|f_{R_k}|} \sum_{o:(f_o \in R_k)} f_o f_o^T \quad (19)$$

where $f_o \in \mathbb{R}^m$ are all descriptors of an image i, $f_o \in R_k$, and $|f_{R_k}|$ denote the descriptors and the corresponding number in the image region R_k, respectively.

A weighted sum of the distance between two images I_i and I_j is

$$D_{\mathrm{LE}}(I_i, I_j) = \sqrt{\sum_{k=1}^{K} w_k (D_{\mathrm{LE}}(X_{i,k}, X_{j,k}))^2} \quad (20)$$

where K is the total number of image regions, $D_{\mathrm{LE}}(X_{i,k}, X_{j,k})$ is the distance between the respective tth image regions of I_i and I_j, and w_k is the weight of the kth region.

The above SPD image descriptors on the LG $\mathbf{G}$ can be transformed to another LG $\mathbf{H}$ by the our proposed algorithm. Then a kernel based on the geodesic distance between two samples in the dimension-reduced LG is defined as

$$K_{\mathrm{LE}}(I_i, I_j) = \exp(-\gamma (D_{\mathrm{LE}}(I_i, I_j))) \quad (21)$$

where the parameter γ is directly related to scaling. It can be easily proved, the same as in [28], that the newly defined LG kernel is a valid Mercer kernel. The LG kernel can be employed in classification methods such as nearest neighbor or SVM.

VI. Experiments

In this section, we evaluate our proposed algorithm by comparing it with several existing state-of-the-art algorithms. We first introduce the experimental setups and then report and analyze the experimental results, after which a further discussion about the effectiveness of the proposed algorithm is given.

A. Experimental Setups

The experiments are conducted on four commonly used datasets: Scene15 [27], Caltech101 [29], UIUC-Sport [10], MIT-Indoor [30], and PASCAL VOC2007 [31].

The Scene15 [27] database consists of 4485 images with 15 categories, each category containing 200–400 images. Following the same experimental setting as in [27], we take 100 images per category for training and the rest images are used for test, and report the averaged classification accuracies over 10 trials.

The Caltech101 [29] contains 8677 images in total, with 102 categories (including one background category). Following the experimental protocol stated by the designers of this dataset, we randomly choose 15 (for the first round) and 30 (for the second round) images per category for training, and use the rest images for test. Then we conduct the

experiment with this random split for 10 times and report the average classification accuracy over these 10 trials for comparison.

The UIUC-Sport dataset [10] has eight complex event classes. Following the sample experiment setting used in [32] and [33], 70 images from each class are randomly sampled for training and 60 images are sampled for test. We run the experiment for 10 trials and report the average classification accuracy.

The MIT-Indoor dataset [30] consists of 67 clustered indoor scene categories, and we adopt the fixed training/testing splits as in [30].

We also use PASCAL VOC2007 dataset [31] to analyze the performances of the proposed method from various aspects. The dataset contains objects of 20 categories and it poses a challenging task of object recognition due to significant variations in terms of appearances and poses even with occlusions. There are 5011 training images and 4952 test images. The performance is evaluated by the standard PASCAL protocol that computes average precision (AP) based on the precision/recall curve; we report the mean AP (mAP) across the 20 categories.

All experiments are conducted based on the following experimental setups.

1) To construct the SPD image features (with no dictionary learning), we extract the 128-D scale-invariant feature transform (SIFT) descriptors, as well as the additional 17-D features including Red Green Blue color values, location, gradient, and the Harris features, via the VLFeat library [45]. Thus, the size of the SPD descriptor $X_i \in \mathcal{S}_m^+$ is 145×145, i.e., $m = 145$.
2) To construct the SPD descriptors, the image is divided into 1×1, 2×2, and 4×4 grids so that totally 21 spatial pooling regions are obtained, assigning the same weight w at the same layer.
3) We empirically set the parameters k_1 and k_2 of the intrinsic graph W_w and the penalty graph W_b in all visual classification experiments, as described in [1]. Specifically, we sample five values $\{2, 3, 5, 7, 9\}$ of k_1 and choose the value with the best performance. We similarly choose the best k_2 in the set $\{20, 40, 60, 80\}$.
4) A one-versus-all scheme is used to tackle the multiclass problem, and the SVM training and testing are performed using the Library Support Vector Machine software package [46]. The parameter γ of the LG kernel is set to 0.001 in our experiment.
5) The dimension n of dimension-reduced data $Y_i \in \mathcal{S}_m^+$ is selected in the set $n = \{145, 135, 125, 115, 105\}$. In our experiment, the best results are reported with $n = 125$.
6) To evaluate the effectiveness of our proposed algorithm, we design a LG kernel method over the original data space without using the proposed algorithm for preprocessing, and we denote this method as LG (without discriminative analysis). The dimension m of the original SPD data X_i is 145.
7) The SPD matrices in the matrix log operation should meet some conditions. Following the same setting defined in [9], we also added a small constant on their diagonal (0.001 in all experiments) for numerical stability.

TABLE I
PERFORMANCE COMPARISON ON THE SCENE15 DATABASE

Method	Accuracy (%)
Li.P *et al.* [7]	80.92±0.44
Lazebnik *et al.* [27]	81.4±0.5
Kwitt *et al.* [34]	82.3
Li *et al.* [35]	85.4
Kobayashi *et al.* [36]	85.63±0.67
Sun *et al.* [37]	86.0±0.8
Fernando *et al.* [38]	86.2±0.4
Zheng *et al.* [39]	86.3
LG	88.02±0.47
Ours	**89.88±0.46**

TABLE II
PERFORMANCE COMPARISON ON THE CALTECH101 DATABASE

Method	Accuracy (%)	
	15 tr.	30 tr.
McCann *et al.* [40]	66.1±1.1	71.9±0.6
Zhang *et al.* [32]	-	75.02±0.74
Sun *et al.* [37]	-	78.8±0.5
Nguyen *et al.* [41]	69.5	77.3
Goh *et al.* [42]	71.1±1.3	78.9±1.1
Duchenne *et al.* [43]	75.3±0.7	80.3±1.2
Feng *et al.* [33]	70.3	82.6
LG	75.83±0.7	81.41±0.9
Ours	**77.42±0.9**	**83.69±0.8**

B. Performance Comparison

Table I shows the classification accuracy on the Scene15 database. It can be seen that the discriminative analysis for SPD matrices on LGs significantly outperforms the others including the log-Euclidean kernel method with sparse representation and dictionary learning of SPD matrices [7], spatial pyramid matching (SPM) [27], SPM on the semantic manifold [34], mid-level visual concepts [35], discriminative part detectors learning method [37], and so on. The LG and our proposed methods are both better than the other methods, and the discriminative analysis for SPD matrices on LGs performs the best when the dimension n of the transformed data $\mathcal{S}_+^n$ is 125. Furthermore, the proposed method improves the performance by 1.86% over the LG kernel method, which does not perform transformation between LGs.

The experimental results on the Caltech101 database are shown in Table II. We compare the proposed method with the exiting algorithms such as low-rank sparse coding [32], sparse embedding [41], kernel sparse representation [42], and so on. The results indicate that our algorithm is significantly better than the other methods. The classification accuracy of the proposed method is 1.6% and 2.28% higher than the result of the LG method for 15 and 30 training images, respectively.

Tables III and IV show the comparison results on the UIUC-Sport and MIT-Indoor datasets, respectively. Our proposed method effectively works compared with the other methods (e.g., kernel sparse representation [42], discriminative part detectors learning method [37] and the LG method).

TABLE III
PERFORMANCE COMPARISON ON THE UIUC-SPORT DATABASE

Method	Accuracy (%)
LiJia *et al.* [10]	76.3
Kwitt *et al.* [34]	83.0
Sun *et al.* [37]	86.4±0.88
Zheng *et al.* [39]	87.2
Zhang *et al.* [32]	88.17±0.85
Li *et al.* [35]	88.4
LG	89.0±1.2
Ours	**90.91±0.9**

TABLE IV
PERFORMANCE COMPARISON ON THE MIT-INDOOR DATABASE

Method	Accuracy (%)
Quattoni *et al.* [30]	26
LiJia *et al.* [10]	37.6
Kwitt *et al.* [34]	44.0
Zheng *et al.* [39]	47.2
Sun *et al.* [37]	51.4
Li *et al.* [35]	52.3
LG	53.46
Ours	**55.58**

TABLE V
MAPS ON PASCAL VOC 2007 DATABASE. PLEASE SEE THE TEXT FOR DETAILS ABOUT EACH METHOD

Method	mAP (in %)
IFK (SIFT) [44]	58.3
Best of VOC07 [31]	59.4
BoF+HOG [36]	59.82
FLH [38]	60.4
IFK (SIFT+Color) [44]	61.7
FLH+BOW [38]	62.8
FK+VC [35]	62.9
LG	61.83
Ours	**63.37**

The classification accuracies of UIUC-Sport and MIT-Indoor datasets are substantially improved from 88.4% and 52.3% (the best reported results [35]) to 90.90 and 55.57, respectively.

Finally, we compare in Table V the result of our proposed algorithm with some results in [31], [35], [36], [38], and [44] on the PASCAL VOC 2007 database. The best method during the PASCAL VOC 2007 competition (by Institut national de recherche en informatique et en automatique) [31] reported 59.4% mAP with multiple channels and costly nonlinear SVMs. Fernando *et al.* [38] obtained an mAP of 60.4% with the method of frequent local histograms (FLH) alone and got an mAP of 62.8% after combining FLH with bag-of-visual-words of SIFT-128 and 5K visual word vocabulary. In [44], improved Fisher kernel (IFK) obtained two results 58.3% and 61.7% with SIFT features only and with SIFT and color information, respectively. Kobayashi [36] reported the 59.83 % mAP by combining bag-of-feature with histogram of oriented gradients. The method combining the IFK with our visual concepts (FK+VC) [35] got an mAP of 62.9%. The proposed method is comparable with some exiting methods, and thus we can say that the method effectively works for the problem of multilabel image classification.

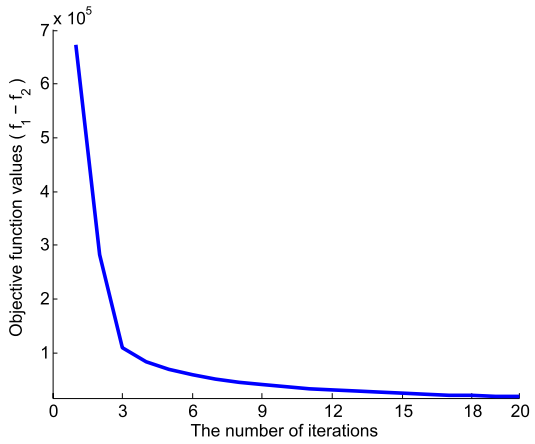

Fig. 3. Relationship between number of iterations and objective function values $f_1 - f_2$ on the Scene15 database.

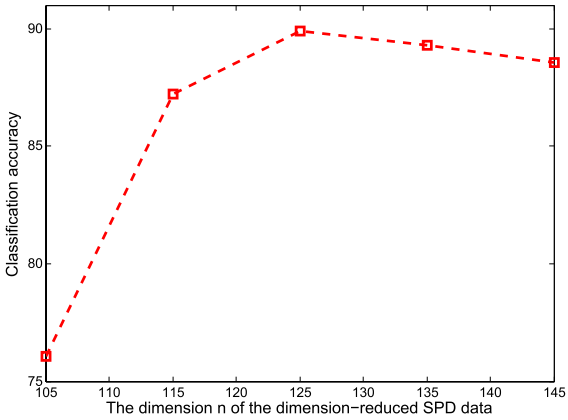

Fig. 4. Relationship between feature dimension and recognition rate on the Scene15 database.

C. Algorithm Analysis

Our proposed algorithm has a fast convergence of the iterations when learning a discriminative transformation in (16). In Fig. 3, we show the relationship between the objective function values $f_1 - f_2$ and the number of iterations on the Scene15 database, namely, how the objective function $f_1 - f_2$ changes with respect to the number of iterations on the Scene15 database.

We then analyze the sensitivity of our proposed algorithm to the different dimensions n of the transformed SPD descriptors. As shown in Fig. 4, different n values have different impact on the classification rates. Due to the redundancy of the manifold-valued data, the discriminative power is limited in the original space of the SPD data. It is noticed that the classification accuracy of the 125-D data is better than the original space of the SPD data ($n = 145$), but the accuracy rate is reduced when the dimension n of the SPD data is 105. If the dimension of the SPD data is very low, the discriminative information may be not sufficient. Therefore, the discriminative power of the data is better only if the dimension of the SPD data is appropriate.

Here, we also analyze the effectiveness of the proposed algorithm with respect to the within-class compactness and the between-class separability on the Scene15 database.

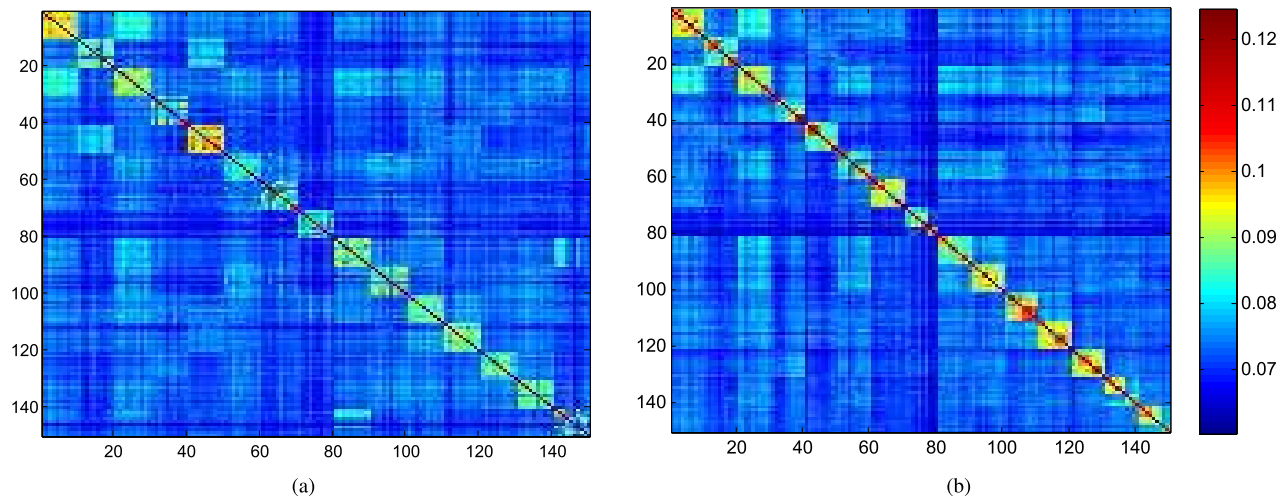

Fig. 5. Affinity matrices derived by (a) LG with no discriminative analysis and (b) our method on the Scene15 database.

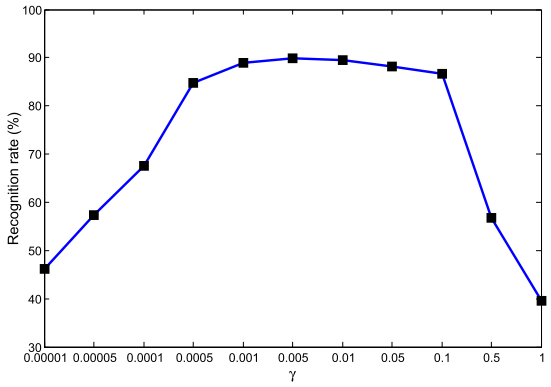

Fig. 6. Performance on the Scene15 database for various parameter γ values of the LG kernel.

We randomly select 10 images per category with scene labels, then order them according to their labels, and test our algorithm on this subset. The derived affinity matrices by the LG method and our proposed method are shown in Fig. 5. We can see that the discriminative analysis for SPD matrices on LGs obtains an affinity matrix that is closer to block diagonal by a discriminative transformation.

Fig. 6 presents the relationship between the discriminative power and the parameter γ on the Scene15 database. The recognition rate is robust as long as the value of the parameter γ falls in the range of approximately from 0.0005 to 0.1; however, the LG kernel with a smaller value of the parameter γ from 0.1 to 1 can significantly deteriorate the recognition rates.

VII. Conclusion

In this paper, we proposed discriminative analysis for SPD matrices on LGs by transforming a LG into a dimension-reduced one. Within the graph embedding framework, a discriminative transformation is learned by optimizing the data separability. This will reduce the cost of model training and testing in pattern analysis. The experimental results show that the proposed method achieves superior performances by comparing with state-of-the-art methods.

The main shortcoming of the proposed approach is costly computation time. Take the UIUC-Sport dataset as an example, the training stage takes around 8 h, while the testing time is about 1 h on an Intel Core 2 Quad processor with 2.83-GHz CPU and 8-GM RAM. Therefore, we shall study how to speed up our proposed manifold learning algorithm for SPD matrices in the future.

Appendix A
Proof of (14) and (15)

Using the transformation function $\log(Y_i) = P^T \log(X_i) P$, we have

$$\begin{aligned}
f_1 &= \sum_{i,j} || \log(Y_i) - \log(Y_j) ||_F^2 W_{ij}^w \\
&= \sum_{i,j} || P^T \log(X_i) P - P^T \log(X_j) P ||_F^2 W_{ij}^w \\
&= \sum_{i,j} \mathrm{tr}\big(\big(P^T \log(X_i) P - P^T \log(X_j) P \big)^T \\
&\qquad \times \big(P^T \log(X_i) P - P^T \log(X_j) P \big) \big) W_{ij}^w \\
&= \sum_{i,j} \mathrm{tr}\big(\big(P^T \log(X_i) P - P^T \log(X_j) P \big) \\
&\qquad \times \big(P^T \log(X_i) P - P^T \log(X_j) P \big) \big) W_{ij}^w \\
&= \sum_{i,j} \mathrm{tr}\big(P^T \log(X_i) P P^T \log(X_i) P \\
&\qquad - P^T \log(X_i) P P^T \log(X_j) P \\
&\qquad - P^T \log(X_j) P P^T \log(X_i) P \\
&\qquad + P^T \log(X_j) P P^T \log(X_j) P \big) W_{ij}^w \\
&= 2 \sum_{i,j} \mathrm{tr}\big(P^T \log(X_i) P P^T \log(X_i) P \\
&\qquad - P^T \log(X_i) P P^T \log(X_j) P \big) W_{ij}^w .
\end{aligned}$$

Similarly

$$\begin{aligned} f_2 &= \sum_{i,j} ||\log(Y_i) - \log(Y_j)||_F^2 W_{ij}^b \\ &= 2\sum_{i,j} \mathrm{tr}\big(P^T \log(X_i) P P^T \log(X_i) P \\ &\qquad - P^T \log(X_i) P P^T \log(X_j) P\big) W_{ij}^b. \end{aligned}$$

APPENDIX B
PROOF OF (17)

Differentiating the objective function f_1 with respect to the transformation matrix P yields

$$\begin{aligned} \frac{\partial \widetilde{f}_1}{\partial P} &= 2\sum_{i,j} \mathrm{tr}\big(4\log(X_i) P P^T \log(X_i) P \\ &\qquad - 2\log(X_i) P P^T \log(X_j) P \\ &\qquad - 2\log(X_j) P P^T \log(X_i) P\big) W_{ij}^w \\ &= 8\sum_{i,j} \big(\log(X_i) P P^T \log(X_i) P \\ &\qquad - \log(X_i) P P^T \log(X_j) P\big) W_{ij}^w. \end{aligned} \tag{22}$$

Similarly

$$\begin{aligned} \frac{\partial \widetilde{f}_2}{\partial P} &= 8\sum_{i,j} \big(\log(X_i) P P^T \log(X_i) P \\ &\qquad - \log(X_i) P P^T \log(X_j) P\big) W_{ij}^b. \end{aligned} \tag{23}$$

Now, combining (22) and (23) gives

$$\begin{aligned} \frac{\partial (f_1 - f_2)}{\partial P} &= 8\sum_{i,j} \big(\log(X_i) P P^T \log(X_i) P \\ &\qquad - \log(X_i) P P^T \log(X_j) P\big)\big(W_{ij}^w - W_{ij}^b\big). \end{aligned} \tag{24}$$

REFERENCES

[1] S. Yan, D. Xu, B. Zhang, H.-J. Zhang, Q. Yang, and S. Lin, "Graph embedding and extensions: A general framework for dimensionality reduction," *IEEE Trans. Pattern Anal. Mach. Intell.*, vol. 29, no. 1, pp. 40–51, Jan. 2007.

[2] M. Moakher and P. G. Batchelor, "Symmetric positive-definite matrices: From geometry to applications and visualization," in *Visualization and Processing of Tensor Fields*. Berlin, Germany: Springer-Verlag, 2006, pp. 285–298.

[3] Y. M. Lui, "Tangent bundles on special manifolds for action recognition," *IEEE Trans. Circuits Syst. Video Technol.*, vol. 22, no. 6, pp. 930–942, Jun. 2012.

[4] C.-Y. Lu, H. Min, Z.-Q. Zhao, L. Zhu, D.-S. Huang, and S. Yan, "Robust and efficient subspace segmentation via least squares regression," in *Proc. ECCV*, 2012, pp. 347–360.

[5] V. Arsigny, P. Fillard, X. Pennec, and N. Ayache, "Geometric means in a novel vector space structure on symmetric positive-definite matrices," *SIAM J. Matrix Anal. Appl.*, vol. 29, no. 1, pp. 328–347, 2006.

[6] S. Jayasumana, R. Hartley, M. Salzmann, H. Li, and M. Harandi, "Kernel methods on the Riemannian manifold of symmetric positive definite matrices," in *Proc. IEEE Conf. CVPR*, Jun. 2013, pp. 73–80.

[7] P. Li, Q. Wang, W. Zuo, and L. Zhang, "Log-Euclidean kernels for sparse representation and dictionary learning," in *Proc. IEEE ICCV*, Dec. 2013, pp. 1601–1608.

[8] O. Tuzel, F. Porikli, and P. Meer, "Region covariance: A fast descriptor for detection and classification," in *Proc. ECCV*, 2006, pp. 589–600.

[9] J. Carreira, R. Caseiro, J. Batista, and C. Sminchisescu, "Semantic segmentation with second-order pooling," in *Proc. ECCV*, 2012, pp. 430–443.

[10] E. P. Xing, L.-J. Li, H. Su, and L. Fei-Fei, "Object bank: A high-level image representation for scene classification & semantic feature sparsification," in *Advances in Neural Information Processing Systems 23*. Red Hook, NY, USA: Curran Associates Inc., 2010, pp. 1378–1386.

[11] V. Arsigny, P. Fillard, X. Pennec, and N. Ayache, "Log-Euclidean metrics for fast and simple calculus on diffusion tensors," *Magn. Reson. Med.*, vol. 56, no. 2, pp. 411–421, 2006.

[12] X. Pennec, P. Fillard, and N. Ayache, "A Riemannian framework for tensor computing," *Int. J. Comput. Vis.*, vol. 66, no. 1, pp. 41–66, 2006.

[13] A. Cherian, S. Sra, A. Banerjee, and N. Papanikolopoulos, "Jensen-Bregman LogDet divergence with application to efficient similarity search for covariance matrices," *IEEE Trans. Pattern Anal. Mach. Intell.*, vol. 35, no. 9, pp. 2161–2174, Sep. 2013.

[14] Z. Wang and B. C. Vemuri, "An affine invariant tensor dissimilarity measure and its applications to tensor-valued image segmentation," in *Proc. IEEE Conf. CVPR*, vol. 1. Jun./Jul. 2004, pp. 228–233.

[15] O. Tuzel, F. Porikli, and P. Meer, "Pedestrian detection via classification on Riemannian manifolds," *IEEE Trans. Pattern Anal. Mach. Intell.*, vol. 30, no. 10, pp. 1713–1727, Oct. 2008.

[16] R. Vemulapalli, J. K. Pillai, and R. Chellappa, "Kernel learning for extrinsic classification of manifold features," in *Proc. IEEE Conf. CVPR*, Jun. 2013, pp. 1782–1789.

[17] J. Ye, R. Janardan, C. H. Park, and H. Park, "An optimization criterion for generalized discriminant analysis on undersampled problems," *IEEE Trans. Pattern Anal. Mach. Intell.*, vol. 26, no. 8, pp. 982–994, Aug. 2004.

[18] S. Yan, Y. Hu, D. Xu, H.-J. Zhang, B. Zhang, and Q. Cheng, "Nonlinear discriminant analysis on embedded manifold," *IEEE Trans. Circuits Syst. Video Technol.*, vol. 17, no. 4, pp. 468–477, Apr. 2007.

[19] J. Hamm and D. D. Lee, "Grassmann discriminant analysis: A unifying view on subspace-based learning," in *Proc. 25th ICML*, 2008, pp. 376–383.

[20] M. T. Harandi, C. Sanderson, S. Shirazi, and B. C. Lovell, "Graph embedding discriminant analysis on Grassmannian manifolds for improved image set matching," in *Proc. IEEE Conf. CVPR*, Jun. 2011, pp. 2705–2712.

[21] P. Li, Q. Wang, and L. Zhang, "A novel earth mover's distance methodology for image matching with Gaussian mixture models," in *Proc. IEEE ICCV*, Dec. 2013, pp. 1689–1696.

[22] R. Wang, H. Guo, L. S. Davis, and Q. Dai, "Covariance discriminative learning: A natural and efficient approach to image set classification," in *Proc. IEEE Conf. CVPR*, Jun. 2012, pp. 2496–2503.

[23] O. Tuzel, F. Porikli, and P. Meer, "Learning on Lie groups for invariant detection and tracking," in *Proc. IEEE Conf. CVPR*, Jun. 2008, pp. 1–8.

[24] C. Chevalley, *Theory of Lie Groups*. Princeton, NJ, USA: Princeton Univ. Press, 1999.

[25] J. Goldbergerm, S. Roweis, G. Hinton, and R. Salakhutdinov, "Neighbourhood components analysis," in *Advances in Neural Information Process*. Toronto, ON, Canada: Univ. Toronto, 2004, pp. 513–520.

[26] S. Boyd and L. Vandenberghe, *Convex Optimization*. New York, NY, USA: Cambridge Univ. Press, 2004.

[27] S. Lazebnik, C. Schmid, and J. Ponce, "Beyond bags of features: Spatial pyramid matching for recognizing natural scene categories," in *Proc. IEEE Conf. CVPR*, Jun. 2006, pp. 2169–2178.

[28] M. Yang, L. Zhang, S. C.-K. Shiu, and D. Zhang, "Robust kernel representation with statistical local features for face recognition," *IEEE Trans. Neural Netw. Learn. Syst.*, vol. 24, no. 6, pp. 900–912, Jun. 2013.

[29] L. Fei-Fei, R. Fergus, and P. Perona, "Learning generative visual models from few training examples: An incremental Bayesian approach tested on 101 object categories," in *Proc. Conf. CVPRW*, Jun. 2004, p. 178.

[30] A. Quattoni and A. Torralba, "Recognizing indoor scenes," in *Proc. IEEE Conf. CVPR*, Jun. 2009, pp. 413–420.

[31] M. Everingham, L. Van Gool, C. K. I. Williams, J. Winn, and A. Zisserman. (2007). *The PASCAL Visual Object Classes Challenge 2007 (VOC2007) Results*. [Online]. Available: http://www.pascal-network.org/challenges/VOC/voc2007/workshop/index.html

[32] T. Zhang, B. Ghanem, S. Liu, C. Xu, and N. Ahuja, "Low-rank sparse coding for image classification," in *Proc. ICCV*, 2013, pp. 281–288.

[33] J. Feng, B. Ni, Q. Tian, and S. Yan, "Geometric ℓ_p-norm feature pooling for image classification," in *Proc. IEEE Conf. CVPR*, Jun. 2011, pp. 2609–2704.

[34] R. Kwitt, N. Vasconcelos, and N. Rasiwasia, "Scene recognition on the semantic manifold," in *Proc. 12th ECCV*, 2012, pp. 359–372.

[35] Q. Li, J. Wu, and Z. Tu, "Harvesting mid-level visual concepts from large-scale internet images," in *Proc. IEEE Conf. CVPR*, Jun. 2013, pp. 851–858.

[36] T. Kobayashi, "BFO meets HOG: Feature extraction based on histograms of oriented p.d.f. gradients for image classification," in *Proc. IEEE Conf. CVPR*, Jun. 2013, pp. 747–754.
[37] J. Sun and J. Ponce, "Learning discriminative part detectors for image classification and cosegmentation," in *Proc. IEEE ICCV*, Dec. 2013, pp. 3400–3407.
[38] B. Fernando, E. Fromont, and T. Tuytelaars, "Effective use of frequent itemset mining for image classification," in *Proc. 12th ECCV*, 2012, pp. 214–227.
[39] Y. Zheng, Y.-G. Jiang, and X. Xue, "Learning hybrid part filters for scene recognition," in *Proc. 12th ECCV*, 2012, pp. 172–185.
[40] S. McCann and D. G. Lowe, "Local naive Bayes nearest neighbor for image classification," in *Proc. IEEE Conf. CVPR*, Jun. 2012, pp. 3650–3656.
[41] H. V. Nguyen, V. M. Patel, N. M. Nasrabadi, and R. Chellappa, "Sparse embedding: A framework for sparsity promoting dimensionality reduction," in *Proc. 12th ECCV*, 2012, pp. 414–427.
[42] S. Gao, I. W.-H. Tsang, and L.-T. Chia, "Kernel sparse representation for image classification and face recognition," in *Proc. 11th ECCV*, 2010, pp. 1–14.
[43] O. Duchenne, A. Joulin, and J. Ponce, "A graph-matching kernel for object categorization," in *Proc. IEEE ICCV*, Nov. 2011, pp. 1792–1799.
[44] F. Perronnin, J. Sánchez, and T. Mensink, "Improving the Fisher kernel for large-scale image classification," in *Proc. 11th ECCV*, 2010, pp. 143–156.
[45] A. Vedaldi and B. Fulkerson. (2008). *VLFeat: An Open and Portable Library of Computer Vision Algorithms*. [Online]. Available: http://www.vlfeat.org/
[46] C.-C. Chang and C.-J. Lin, "LIBSVM: A library for support vector machines," *ACM Trans. Intell. Syst. Technol.*, vol. 2, no. 3, pp. 27:1–27:27, 2011.

Chunyan Xu received the B.Sc. degree from Shandong Normal University, Jinan, China, in 2007, and the M.Sc. degree from Huazhong Normal University, Wuhan, China, in 2010. She is currently working toward the Ph.D. degree with the School of Computer Science and Technology, Huazhong University of Science and Technology, Wuhan, and the Department of Electrical and Computer Engineering, National University of Singapore, Singapore.

Her research interests include computer vision, manifold learning, and kernel methods.

Canyi Lu received the bachelor's degree in mathematics from Fuzhou University, Fuzhou, China, in 2009 and the master's degree in pattern recognition and intelligent systems, in 2012. He is currently working toward the Ph.D. degree with the Department of Electrical and Computer Engineering, National University of Singapore, Singapore.

His research interests include computer vision and machine learning.

Junbin Gao received the B.Sc. degree in computational mathematics from Huazhong University of Science and Technology (HUST), Wuhan, China, in 1982, and the Ph.D. degree from Dalian University of Technology, Dalian, China, in 1991.

He was an Associate Lecturer, a Lecturer, an Associate Professor, and a Professor with the Department of Mathematics, HUST, from 1982 to 2001. He was a Senior Lecturer and Lecturer in Computer Science with University of New England, Armidale, NSW, Australia, from 2001 to 2005. He is currently a Professor of Computing Science with the School of Computing and Mathematics, Charles Sturt University, Bathurst, NSW, Australia. His research interests include machine learning, data mining, Bayesian learning and inference, and image analysis.

Wei Zheng received the bachelor's degree from Tsinghua University, Beijing, China, in 2006 and the Ph.D. degree from the Institute of Computing Technology, Chinese Academy of Sciences, Beijing, in 2013.

He is a Researcher with the Beijing Samsung Telecom Research and Development Center, Beijing. His research interests include image categorization, object detection, and scene analysis.

Tianjiang Wang received the B.Sc. degree in computational mathematics and the Ph.D. degree in computer science from Huazhong University of Science and Technology (HUST), Wuhan, China, in 1982 and 1999, respectively.

He is a Professor with the School of Computer Science, HUST. He has finished some related projects and has authored over 20 related papers. His research interests include machine learning, computer vision, and data mining.

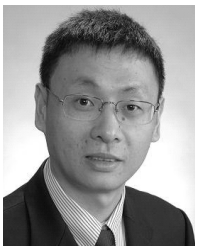

Shuicheng Yan is an Associate Professor with the Department of Electrical and Computer Engineering, National University of Singapore (NUS), Singapore, and the Founding Lead of the Learning and Vision Research Group. He was an ISI Highly-Cited Researcher in 2014. He has authored or co-authored 100 technical papers over a wide range of research topics, with the Google Scholar citation over 15 000 times and an H-index of 51. His research interests include machine learning, computer vision, and multimedia.

Dr. Yan was a fellow of the International Association for Pattern Recognition in 2014. He received the best paper awards from the ACM Multimedia (MM) (best paper and best student paper) in 2013, ACM MM Best Demo in 2012, the Pacific-Rim Conference on Multimedia in 2011, ACM MM in 2010, the International Conference on Multimedia and Expo in 2010, and the International Conference on Internet Multimedia Computing and Service in 2009, the Runner-Up Prize of the ImageNet Large Scale Visual Recognition Challenge (ILSVRC) in 2013, the winner prize of the detection task in ILSVRC in 2014, the winner prizes of the classification task in PASCAL VOC from 2010 to 2012, the winner prize of the segmentation task in PASCAL VOC in 2012, the honorable mention prize of the detection task in PASCAL VOC in 2010, IEEE TRANSACTIONS ON CIRCUITS AND SYSTEMS FOR VIDEO TECHNOLOGY Best Associate Editor Award in 2010, the Young Faculty Research Award in 2010, the Singapore Young Scientist Award in 2011, and the NUS Young Researcher Award in 2012. He has served as an Associate Editor of IEEE TRANSACTIONS ON KNOWLEDGE AND DATA ENGINEERING, IEEE TRANSACTIONS ON CIRCUITS AND SYSTEMS FOR VIDEO TECHNOLOGY, and *ACM Transactions on Intelligent Systems and Technology*.